Protein Science (2000), *9*:1960–1967. Cambridge University Press. Printed in the USA.

Formation of insulin amyloid fibrils followed by FTIR simultaneously with CD and electron microscopy

MARIO BOUCHARD, JESÚS ZURDO, EWAN J. NETTLETON, CHRISTOPHER M. DOBSON, AND CAROL V. ROBINSON

Oxford Centre for Molecular Sciences, New Chemistry Laboratory, University of Oxford, South Parks Road, Oxford OX1 3QT, United Kingdom

(RECEIVED February 14, 2000; FINAL REVISION May 30, 2000; ACCEPTED July 14, 2000)

Abstract

Fourier transform infrared spectroscopy (FTIR), circular dichroism (CD), and electron microscopy (EM) have been used simultaneously to follow the temperature-induced formation of amyloid fibrils by bovine insulin at acidic pH. The FTIR and CD data confirm that, before heating, insulin molecules in solution at pH 2.3 have a predominantly native-like α-helical structure. On heating to 70 °C, partial unfolding occurs and results initially in aggregates that are shown by CD and FT-IR spectra to retain a predominantly helical structure. Following this step, changes in the CD and FTIR spectra occur that are indicative of the extensive conversion of the molecular conformation from α-helical to β-sheet structure. At later stages, EM shows the development of fibrils with well-defined repetitive morphologies including structures with a periodic helical twist of ~450 Å. The results indicate that formation of fibrils by insulin requires substantial unfolding of the native protein, and that the most highly ordered structures result from a slow evolution of the morphology of the initially formed fibrillar species.

Keywords: CD; electron microscopy; fibril formation; FTIR; insulin; X-ray diffraction

The amyloid diseases, which include Alzheimer's disease, the spongiform encephalopathies and type II diabetes, are characterized by the abnormal self-assembly and deposition of proteinaceous material into insoluble ordered aggregates (Sipe, 1992; Tan & Pepys, 1994; Pepys, 1996; Kelly, 1998; Dobson, 1999). So far, nearly 20 different amyloidogenic precursors have been identified although the detailed mechanism underlying the formation of fibrils by these proteins remains unclear at a molecular level (Sipe, 1994; Tan & Pepys, 1994; Pepys, 1996; Sunde & Blake, 1997). A number of biophysical studies, however, support the idea that a population of unfolded or partially folded intermediates may be a fundamental characteristic that links the diverse amyloid-associated disorders (Taubes, 1996; Booth et al., 1997; Kelly, 1998). For example, studies of transthyretin (both wild-type and amyloidogenic variants) and amyloidogenic variants of lysozyme highlight the requirement of conformational changes for the conversion from native protein molecules into amyloid fibrils (Colon & Kelly, 1992; Lai et al., 1996; Booth et al., 1997; Nettleton et al., 1998; Canet et al., 1999). Under partially denaturing conditions in vitro, these and other amyloidogenic species are capable of self-assembly into amyloid fibrils. Moreover, the formation of amyloid fibrils has been suggested to be a generic property of peptides and proteins and not one restricted to the particular species observed in disease states (Guijarro et al., 1998; Chiti et al., 1999; Dobson, 1999).

An understanding of the various processes leading to the formation of amyloid fibrils and of the conformational properties of the unfolded or partially structured precursors is essential to understand fully the mechanism of amyloid deposition. A necessary step in this process is the elucidation of the molecular structure of the fibrils themselves. A variety of methods of structural analysis has been applied to fibrils from a range of proteins. X-ray diffraction has been extensively applied for the structural characterization of amyloid and resulted in a model of the structure of a common core protofilament composed of elements of β-sheets (Sunde & Blake, 1997). These sheets run parallel to the axis of the fibril, with their component β-strands perpendicular to this axis. The β-sheets twist around a common helical axis that coincides with the axis of the protofilament. A recent study has demonstrated an alternative approach to obtaining a detailed molecular view of fibrils by using cryo-electron microscopy coupled with image processing and reconstruction techniques. These processes have been applied to fibrils produced from the SH3 domain of phosphatidylinositol-3′-kinase, indicating that these fibrils have four protofilaments, each protofilament consisting of a pair of flat untwisted β-sheets (Jiménez et al., 1999). All the structural studies reveal the importance of hydrogen bonding interactions between extensive regions of the polypeptide backbone.

Reprint requests to: Carol V. Robinson, University of Oxford, Oxford Centre for Molecular Sciences, New Chemistry Laboratory, South Parks Road, Oxford OX1 3QT, United Kingdom; e-mail: carolr@bioch.ox.ac.uk.

Abbreviations: CD, circular dichroism; FTIR, Fourier transform infrared spectroscopy; EM, electron microscopy.

Insulin is a small helical protein hormone consisting of two polypeptides, chain A (21 residues) and chain B (30 residues), linked together by two interchain disulfide bridges. X-ray analysis of the hexamer reveals that chain A consists of two helical segments, A2–A8 and A13–A20, chain B includes a region of extended structure B1–B8, an α-helical region between residues B9–B19, a β-turn, B20–B23, and finally, another extended strand between residues B24–B28 (Blundell et al., 1971). When insulin is heated at high temperature and low pH, a series of structural changes occurs and results in the formation of fibrillar structures (Waugh, 1946; Brange et al., 1997a). In the present work, we explore aspects of the formation of such fibrils by bovine insulin. Specifically, the characteristics of the growth reaction have been followed by a combination of FTIR, CD, and EM to gain insight into the events underlying the structural transformation of a highly helical protein to largely β-sheet amyloid fibrils. As well as providing information that might help to understand the molecular basis of amyloid diseases, a better understanding of the aggregation properties of insulin is important with respect to its long-term stability in commercial pharmaceutical formulations and its utilization in the treatment of diabetes (Sluzky et al., 1992; Brange et al., 1997a; Dodson & Steiner, 1998).

Results

Spectroscopic studies of the conversion of insulin molecules to fibrils

Temperature-induced fibril formation by bovine insulin at 68 °C (2 mM, in D_2O at pD, 2.6) was followed first by CD and FTIR over a period of 7 h. Fibril formation is highly dependent upon the history of the particular sample studied (Brange et al., 1997a). Differences observed in the rate of fibril formation between different samples can be explained by small differences in experimental conditions, such as pH, temperature, and/or salt concentrations. In this study to circumvent this problem both the CD and FTIR experiments at each time point were carried out on the same sample preparation. The CD (panel A) and FTIR (panel B) data for such an experiment are presented in Figure 1. The CD spectrum of insulin before heating shows a double minima at 208 and 222 nm indicative of substantial α-helical structure, consistent with the crystal structure of the insulin hexamer (Blundell et al., 1971) and with an NMR solution structure determined under similar conditions of pH but in the presence of 20% acetic acid (Hua & Weiss, 1991). Moreover, a mass spectrometry experiment in which hydrogen exchange protection in specific residues was measured at pH 2.0 is consistent with the presence of extensive native-like helical structure (Tito et al., 2000). After heating to 68 °C, the CD spectrum of the protein displays a significant decrease in the ellipticity at 222 nm, accompanied by a shift of the minimum at 208 nm toward lower wavelengths. An increase in random coil structure (characterized by a single minimum below 200 nm) can account for the shift of the 208 nm band toward lower values. The loss of intensity of the 222 nm band indicates that the increase in random coil structure is accompanied by a reduction in the α-helical content of the structure. Heating insulin to initiate fibril formation therefore results initially in a partial unfolding of the protein structure. As insulin is heated for longer periods (2 and 7 h), the CD spectrum becomes one that is typical of the presence of extensive β-sheet structures, characterized by a minimum in the ellipticity at 216 nm. As a control experiment, CD spectra were also recorded under the same conditions of temperature and pH but in H_2O. The same structural features were observed.

The FTIR spectra corresponding to each time point for which the CD spectra are shown are also presented in Figure 1. In these experiments, the structural behavior of insulin during fibril growth was monitored by observing changes in the shape and the frequency of the amide I band as a function of time. Before heating,

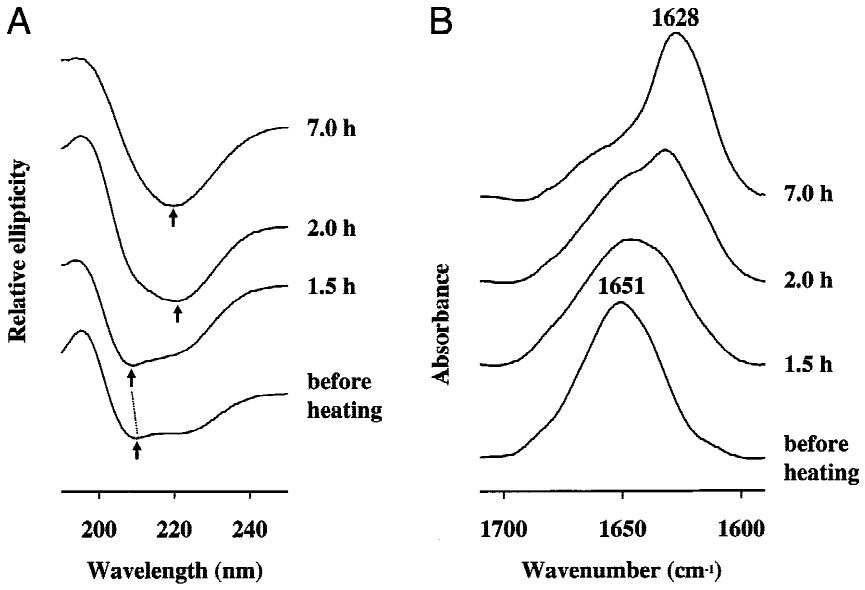

Fig. 1. Time evolution of the (**A**) CD and (**B**) FTIR spectra of insulin (2 mM) during fibril formation at 68 °C and pD 2.6. Spectra were recorded before heating and 1.5, 2, and 7 h after initiation of the heating treatment. The CD and FTIR data shown in this figure have been recorded simultaneously using the same samples. In the CD spectra, the arrows indicate the wavelength of maximum negative ellipticity.

the amide I band is sharp and located at ~1,651 cm^{-1}. The shape and the position of the band are consistent with the presence of largely helical and/or disordered structures (Krimm & Bandekar, 1986; Arrondo et al., 1993; Vecchio et al., 1996). This result is in good agreement with the CD data that clearly show that insulin under the conditions studied here is predominantly α-helical prior to heating.

Following an increase in temperature to 68 °C, we observe a shift of the IR band at ~1,651 cm^{-1} toward lower frequencies and the appearance of a small shoulder on this band. The shift of the band is indicative of the presence of an increased amount of disordered structure and the shoulder of a small amount of β-sheet structure. The CD spectrum corresponding to this time point as discussed above shows that the protein is still largely helical, albeit with an increase in the content of random coil structure. The CD and FTIR results are therefore in good agreement and indicative of the partial unfolding of the protein. In the FTIR, spectra recorded at longer times, 2 and 7 h, we can clearly observe the emergence of bands whose positions (1,627 and ~1,670 cm^{-1}) are strongly indicative of the presence of intermolecular β-sheet and β-turn structures (Krimm & Bandekar, 1986; Halverson et al., 1990; Surewicz et al., 1993). The increase in the band associated with β-sheet structure in the FTIR spectra correlates with the large change in the CD spectra indicative of the formation of β-sheet structure. The FTIR spectrum after this time period indicates, like the CD spectrum, that the sample is largely β-sheet but that residual (up to 10%) α-helical/disordered structure remains.

Structural studies of the species formed during the process of fibril formation

The formation of fibrils under conditions closely similar to those described above was followed in further detail for a longer period of time using a combination of FTIR and EM. The FTIR spectra are shown in Figure 2A. They reveal the same features as described in the previous section and show the α-helical to β-sheet conformational transition, via the formation of disordered structures, that accompanies the formation of the fibrils. The somewhat slower evolution of β-sheet structure in this experiment despite the similar conditions used in Figure 1 reveals the sensitivity of the fibril formation process to the exact history of the sample (Brange et al., 1997a). Further, the spectra show more clearly the presence of a lag phase in the kinetics, a phenomenon well exhibited in studies of fibril formation by other systems (Jarrett & Lansbury, 1993; Harper & Lansbury, 1997).

The α-helix to β-sheet conformational transition can be seen more clearly in the resolution-enhanced second derivative spectra. Figure 2B shows such spectra for insulin before the heat treatment and after 1.5 and 18 h of heating at 70 °C. The spectrum of the protein before heating shows that the protein is in a helical/disordered conformation with bands at ~1,639 and 1,652 cm^{-1}, respectively. Heating the sample for 1.5 h results in a small increase in the content of random coil structure although the protein is still largely helical. Such an observation is in agreement with our interpretation of the CD-FTIR data discussed above. Further, we can also observe in these spectra the presence of peaks associated with antiparallel β-sheet structures (~1,612 and 1,683 cm^{-1}). This structure could be indicative of the presence of some aggregated or fibrillar material prior to the heating treatment (vide infra). The second derivative spectrum of insulin after 18 h of heating at 70 °C shows that the protein has converted almost completely to β-sheet structure. The spectrum exhibits a very strong band at 1,626 cm^{-1}. However, the spectrum does not show any high frequency component (~1,690 cm^{-1}) that would suggest the presence of antiparallel β-sheet (Fabian et al., 1993). We suggest, therefore, that the β-sheet structure in the insulin fibrils could be predominantly parallel rather than antiparallel.

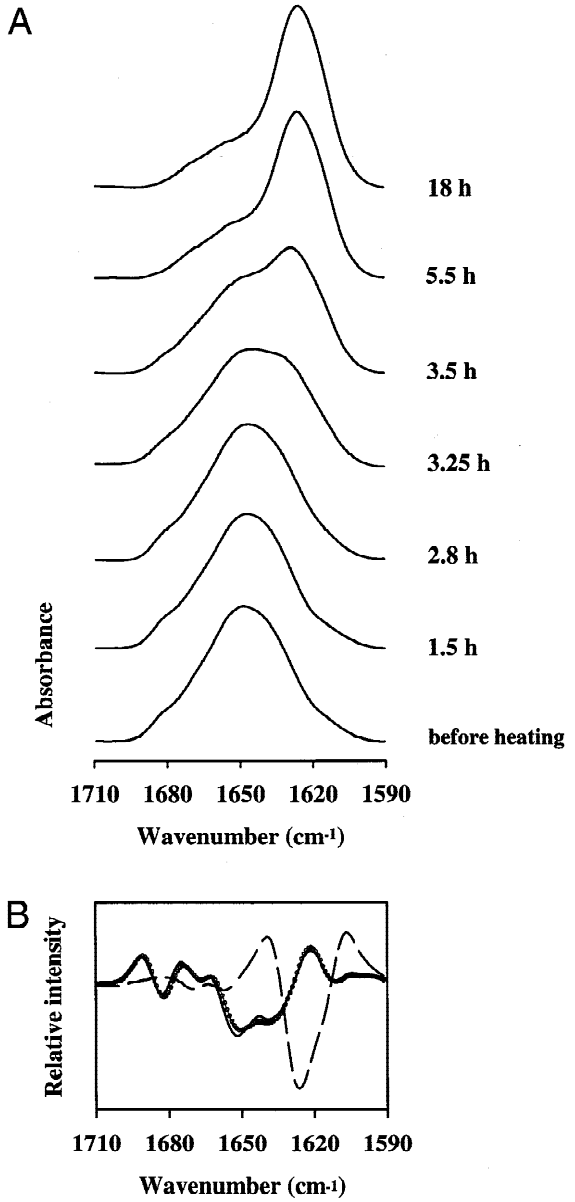

Fig. 2. A: Time evolution of the FTIR spectra of the amide I region of insulin (2 mM) during fibril formation at 70 °C and pD 2.67. Samples were collected before the heating treatment and after initiation of the heating for different periods of time, 1.5, 2.8, 3.25, 3.5, 5.5, and 18 h. Electron micrographs were collected simultaneously for each sample and are shown in Figure 3. **B:** Second derivative spectra of insulin prior to heating (solid line) and after 1.5 h (dotted line) and 18 h (dashed line) of heating at 70 °C.

For each of the samples shown in Figure 2A, an EM picture was recorded (Fig. 3). Distinct time-dependent morphological stages can be observed in these images. Figure 3A shows an electron micrograph of the sample prior to heat treatment. This reveals the

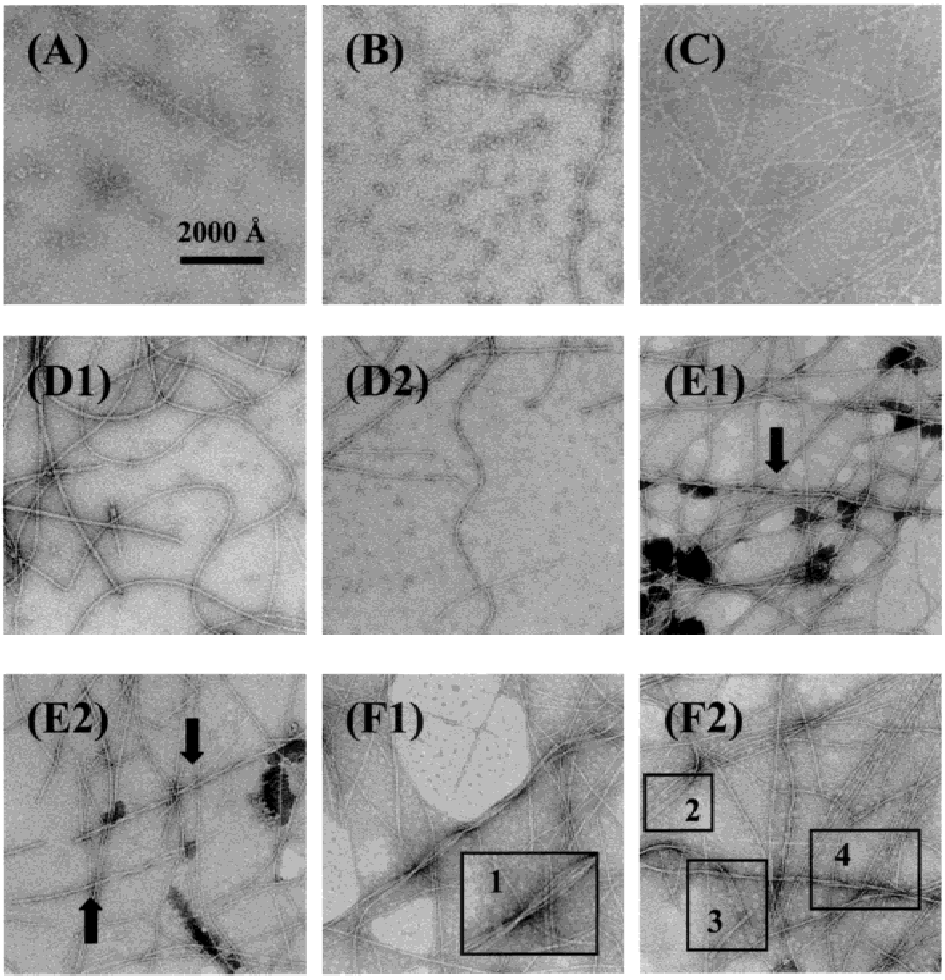

Fig. 3. Time evolution of the electron micrographs of insulin (2 mM) during fibril growth at 70 °C and pD 2.67. Samples were collected before heating **(A)** and after heating for the following periods of time: **(B)** 1.5 h, **(C)** 2.8 h, **(D1, D2)** 3.25 h, **(E1, E2)** 5.5 h, and **(F1, F2)** 18 h. (Bar = 2,000 Å). The samples used in this experiment are the same as for the FTIR spectra shown in Figure 2 but have been diluted (see Materials and methods) so that a quantitative comparison of the number of fibrils in each electron micrograph is not valid.

presence of small clusters of aggregated protein. These aggregates do not have the regular fibrillar appearance associated with amyloid structures. The FTIR spectrum (Fig. 2A) corresponding to this sample shows, as discussed above, that insulin prior to heating is largely helical in structure, a finding consistent with CD spectroscopy (Fig. 1). The state of aggregation of the soluble species present prior to fibril formation cannot be assessed from the data recorded in this study. Mass spectrometry data recorded for insulin solutions under similar conditions prior to fibril formation, however, suggest that the predominant species is likely to be monomeric insulin. A range of higher oligomers was, however, observed and clusters containing up to 12 insulin molecules could be detected in these solutions (Nettleton et al., 2000). The intensities of all the signals in the mass spectra were found to decrease during the incubation period as both the monomeric and oligomeric forms of insulin are depleted. These results are consistent with other studies that show the formation of soluble aggregates of native insulin under similar solution conditions (Hua & Weiss, 1991; Brange et al., 1992). A very small quantity of fibrillar material could be observed by EM in samples prior to the heat treatment. This may be a result of the conversion to fibrils of a very small quantity of protein during sample preparation (see Materials and methods), presumably as a consequence of the procedures used to exchange hydrogen for deuterium for the FTIR experiments. The conditions used for this procedure (low pH) are highly favorable for aggregation and fibril formation (Waugh, 1946).

The electron micrograph taken 1.5 h after initiation of heating is shown in Figure 3B. The micrograph reveals, in addition to an increase in the amount of amorphous aggregated clusters over those present before heating (Fig. 3A), the appearance of a small number of well-defined fibrils. The FTIR spectrum corresponding to this time point shows only a small shift of the band toward lower frequencies indicative of an increase in the proportion of random coil structure. Combination of the EM, CD, and FTIR data, therefore, suggest that insulin fibril formation occurs after the initial formation of aggregates with predominantly native-like structure. Figure 3C shows an electron micrograph of the sample heated for 2.8 h. This reveals the emergence of a network of fibrils in the presence of nonfibrillar aggregates, some of which appear to be associated with the fibrils. There is no evidence as to whether structural reorganization to form fibrils take place within the initially formed aggregates or whether dissociation of insulin mol-

ecules from these structures occurs, and that the fibrils then form by a separate and independent nucleation process. The FTIR spectrum corresponding to this time point shows a small broadening of the amide I band due to an increased contribution of the band at ~1,628 cm^{-1}; this can be correlated with the increased number of fibrils seen in the EM pictures. After an additional 25 min, the clusters of aggregates observed at the surface of the fibrils in Figure 3C can no longer be seen and the fibrils are long, unbranched, smooth, and have a diameter of ~70–90 Å (Figs. 3D1, 3D2). The fibrils also show a high degree of curvature (Fig. 3D2) but show no twisting pattern along the fiber axis. At this point in the FTIR spectrum, we can clearly observe the emergence and dominance of the band characteristic of β-sheet structure.

The micrographs in Figures 3E1 and 3E2 show fibrils obtained after heating the insulin sample for 5.5 h. Two types of assemblies are now evident: one is a smooth, nontwisted fibril of the type observed previously, and the other is a twisted fibril (indicated by the arrows). Fibrils of the latter type, at this stage in their growth, show no defined periodicity in the pattern of their helical twists. Moreover, it is not clear if the twisted fibrils are due to the association of two or more strands or protofilaments or result from the twisting of a single protofilament. However, a direct comparison of the size of the smooth and twisted fibrils suggests that the latter are formed by association of at least two protofilaments. Figures 3F1 and 3F2 show electron micrographs of the sample heated for 18 h. The number of twisted fibrils in relation to others has increased, although a range of morphologies can still be observed. Notably, there are many non-twisted ribbon-like fibrils in addition to the twisted ones. In Figure 3F1, a distinct image of an open twisted ribbon is shown and reveals that at least four protofilaments are wound together to form the fibrils. In Figure 3F2, boxes 2 and 3 show flat ribbon-like fibrils consisting apparently of two and three individual strands, respectively. Box 4 shows the twisted fibrils observed in Figures 3E1 and 3E2 and described above. These observations suggest that different fibrils can contain different numbers of strands or protofilaments. The FTIR spectrum corresponding to the 18 h time point shows an intense band at ~1,628 cm^{-1} indicative of the presence of a large amount of intermolecular β-sheet structure and consistent with the large numbers of fibrils formed (Fabian et al., 1993).

Observation of fibril maturation by EM

Figures 4 and 5 show electron micrographs of an insulin sample in which the fibrils have been allowed to develop for much longer periods of time, 10 and 40 weeks at room temperature, respectively. The fibrils observed after 10 weeks in Figure 4 are highly twisted. Some of these fibrils have a high degree of curvature as observed in Figure 4A. Others are straight and tightly twisted, as shown in Figure 4B, and have a well-defined helical repeat of ~450 Å. Despite these differences, the sample generally shows a higher degree of homogeneity in the fibril morphologies than those described above (Fig. 3). Nevertheless, fibrils with significantly different morphologies can still be observed. Panel 1 in Figure 4C shows a single smooth fibril of the type observed in Figure 3. Such fibrils may be the basic unit of the twisted fibrils observed in Figure 4A and 4B. Association of two fibrils of this type would account for the diameter of the twisted fibrils in their largest cross sections in Figures 4A and 4B. In fact, box 2 of Figure 4C shows a fibril formed by the association of at least two strands or protofilaments. The diameter of this flat ribbon-like fibril is ~140–150 Å, which also corresponds to the diameter of the highly twisted fibrils in their largest sections in Figures 4A and 4B. Twisting of such flat ribbons could therefore give rise to the highly twisted appearance of the fibrils. An electron micrograph of this same sample after 40 weeks is shown in Figure 5A. No dramatic changes are observed in the overall morphologies of the fibrils, which are generally still highly twisted. However, the number of highly twisted fibrils relative to the nontwisted ones has increased significantly compared to the sample examined after 10 weeks suggesting again an evolution of the structure of the fibrils over time. Twisting of the fibrils may well occur because it might enable more effective burial of exposed hydrophobic surfaces, and is also likely to result in increased Van der Waals interactions, leading to greater stability. A similar evolution in the morphology of Alzheimer's β-amyloid peptide fibrils has been observed in a time-dependent EM study

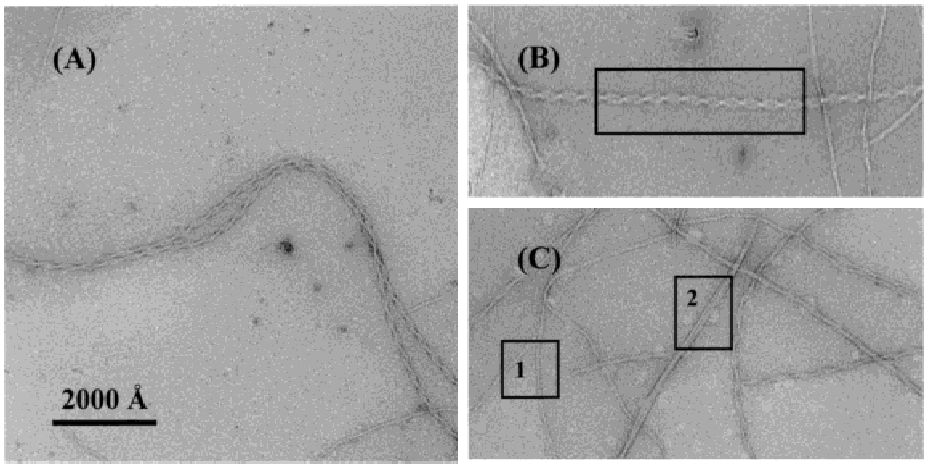

Fig. 4. Selected images of the electron micrographs of an insulin fibril sample incubated for 10 weeks in water at pH 2.27. **A:** Highly twisted curved fibrils. **B:** Highly twisted straight fibril with a twist repeat of ~450 Å. **C:** Different morphologies observed in the sample; box 1 shows a single smooth tubular fibril, box 2 shows the association of at least two strands to form a flat ribbon-like fibril. The dimensions are such that twisting of a flat ribbon of this type could give rise to the type of fibrils observed in **A**. (Bar = 2,000 Å).

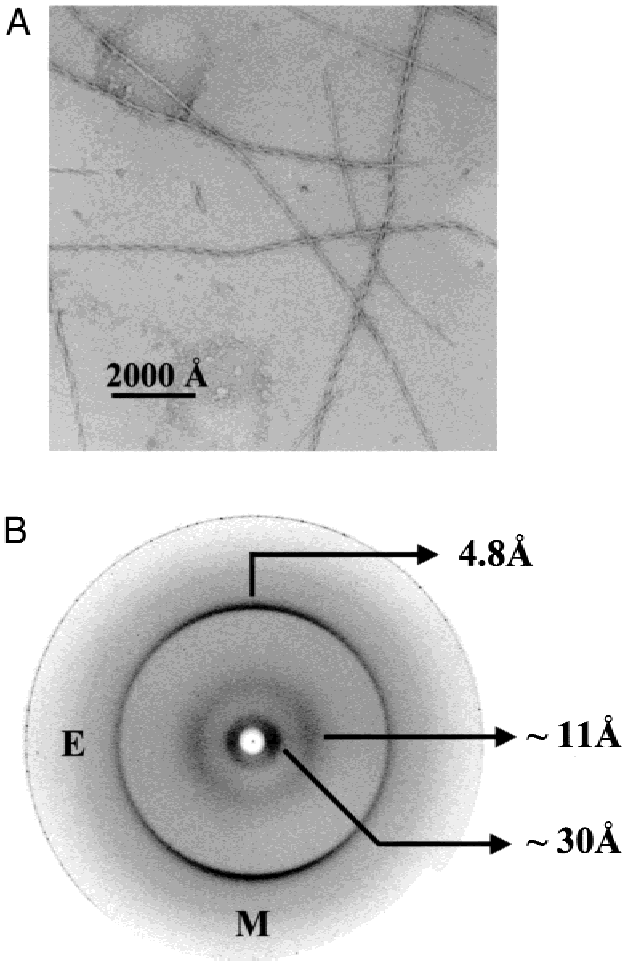

Fig. 5. A: Electron micrograph of the insulin fibril preparation shown in Figure 4 after incubation at room temperature for 40 weeks showing highly twisted fibrils (bar = 2,000 Å). **B:** X-ray diffraction pattern from the sample shown in **A**. The pattern shows dominant reflections at 4.8 Å on the meridian and ~11 and ~30 Å on the equator. (The letters M and E represent the meridional and equatorial axes, respectively.)

(Seilheimer et al., 1997). As in the case of insulin described here, when the fibrils reach a mature state the number of twisted structures is increased.

An X-ray diffraction image of the insulin fibrils produced over a period of 40 weeks is shown in Figure 5B. Three strong reflections can be observed. The dominant reflection is sharp and intense and occurs at 4.8 Å. Two weaker more diffuse but still intense reflections are observed at ~11 and ~30 Å, respectively. The 4.8 and ~11 Å reflections constitute the cross-β pattern that is typical of amyloid fibrils (Sunde & Blake, 1997). The 4.8 Å meridional reflection arises from the spacing between the strands in the β-sheet structure, and the 11 Å equatorial reflection corresponds to the intersheet spacing (Sunde & Blake, 1997). In the case of insulin, the 30 Å equatorial reflection must arise from a structural spacing that is perpendicular to the axis of the fibrils and may be associated with the separation between the protofilaments in the fibrils. The reflections at 4.8, 11, and 30 Å observed in this study are in good agreement with data reported in previous studies of insulin (Koltun et al., 1953; Burke & Rougvie, 1972) and, with the exception of the 30 Å reflection, have been observed in all other amyloid fibril diffraction patterns (Kirschner et al., 1987, 1998; Gilchrist & Bradshaw, 1993; Sunde & Blake, 1997).

Discussion

The combination of experimental observations described here indicates that the formation of fibrils from soluble insulin molecules proceeds in a series of stages. On a macroscopic scale, the different stages can be observed by EM and consist of the formation of nonfibrillar aggregates, the development of protofilaments and their assembly into fibrils, and finally the rearrangement of the fibrils into well-ordered highly twisted structures with a helical repeat of ~450 Å. On a molecular level, the CD and FTIR results show that insulin prior to heat treatment has substantially native-like α-helical characteristics. These spectroscopic observations combined with the results of NMR (Hua & Weiss, 1991) and mass spectrometry studies (Nettleton et al., 2000) indicate that under the solution conditions used in the present study, insulin forms small soluble oligomers of native-like molecules. Following heating there is a lag phase, and the formation of fibrils involves a significant increase in β-sheet structure, as revealed in the CD and FTIR spectra. The presence of aggregates, observed in the EM pictures, prompts the questions as to whether or not structural reorganization of insulin to from fibrils takes place within the larger aggregates observed or whether monomeric insulin dissociates from these structures and gives rise to fibrils. Although there is on evidence for either mechanism from this study, the fact that the intermolecular interactions in amyloid fibrils involve β-strands implies a substantial structural reorganization step to yield a favorable intersheet alignment, presumably optimizing hydrogen bonding and interstrand side-chain interactions. After the fibrils have formed, further reorganization of the initially formed structures takes place to generate highly twisted fibrils. This reorganization may have as a driving force the more effective burial of at least some of the exposed hydrophobic surfaces.

The question arises as to whether the β-sheet structure formed in insulin fibrils results from the assembly of β-strands in a parallel or antiparallel manner or whether both types of structure exist. Both types of structure occur in the native state of globular proteins although the antiparallel arrangement is more common. For insulin fibrils the presence of parallel β-sheets has been suggested from X-ray diffraction studies (Burke & Rougvie, 1972) and antiparallel structure from analysis by Raman spectroscopy (Yu et al., 1974). The proposition that insulin fibrils are composed of dimers of native insulin is also consistent with antiparallel structure (Turnell & Finch, 1992; Brange et al., 1997b). Fibrils formed from the ADA2H domain (Villegas et al., 2000), acylphosphatase (Chiti et al., 1999), and from specific peptides of the β-amyloid protein (Fabian et al., 1993), have been found to exhibit significant intensity at ~1,690 cm^{-1}, indicative of a significant content of antiparallel β-sheet structure. No high frequency band could be observed for insulin after 18 h of heating at 70 °C (see the second derivative spectrum in Fig. 2B). This suggests that the β-sheet structures in insulin fibrils consist largely of parallel β-strands. However, the FTIR analysis is based largely on empirical correlations and further analysis will be necessary to characterize fully the structural arrangement of the β-sheet assemblies formed in the insulin fibrils.

The data presented here for insulin emphasize the close similarities in the process of fibril formation by different proteins, whether disease related or not, such as lysozyme, transthyretin, the

SH3 domain of phosphatidylinositol-3′-kinase and others (Colon & Kelly, 1992; Lai et al., 1996; Booth et al., 1997; Guijarro et al., 1998; Nettleton et al., 1998; Canet et al., 1999). In each case, an unfolded or partially unfolded conformation is involved and in most cases nonfibrillar aggregates have been observed prior to fibril formation. For this conversion, the spectroscopic evidence points to the formation of extensive intermolecular β-sheet structures from a nonnative precursor and not to an alternative well-defined soluble β-form of the proteins. This requirement for aggregation of unfolded rather than native species, for the majority if not all amyloidogenic proteins, may account for the observation of a similar core structure for all amyloid fibrils (Sunde et al., 1997). Moreover, the formation of fibrils by a protein whose secondary structure is largely helical in its soluble form clearly demonstrates that the presence of a substantial intrinsic propensity to form β-structure is not necessary for amyloid formation to occur.

On a practical level, the results of these experimental investigations stress the importance and value of using complementary biophysical techniques to study protein aggregation. Other studies have used FTIR and CD to follow formation of intermolecular β-sheet structure during protein gellation (Dong et al., 1997, 1998; Kendrick et al., 1998). In the present study, we extend this methodology and carry out our experiments on identical samples to enable direct comparisons between the different biophysical techniques. This procedure allows the extreme sensitivity of fibril formation to the solution conditions, and the results of the irreproducible nature of the process, to be overcome in comparing the results of the different techniques. Furthermore the combined use of these techniques allows optimal conditions to be found for the preparation of highly ordered fibrils, an important requirement for high resolution structural studies (Jiménez et al., 1999).

Materials and methods

Materials

Insulin from bovine pancreas was purchased from Sigma Chemical Co. (St. Louis, Missouri) and used without further purification. D_2O and DCl were obtained from Fluorochem Limited (Azusa, California) and Sigma Chemical Co., respectively.

Samples for FTIR

Exchangeable hydrogens in insulin were replaced by deuterons by dissolving the protein in D_2O (2.0 mM) at pD 1.9, leaving the sample at room temperature for 12 h followed by lyophilization. This procedure was repeated until the labile hydrogens in the sample were completely replaced by deuterons ($\geq$98% exchange). The extent of deuteration was analyzed by nanoflow electrospray mass spectrometry using a Platform II mass spectrometer (Micromass UK Ltd., Manchester, U.K.). The pD of the solution was adjusted with dilute DCl solution. The final concentration of insulin was 2 mM.

Formation of fibrils

A 2.0 mM deuterated insulin solution at pD $\sim$2.67 was heated to $\sim$70 °C. When the sample was left at this temperature for even short times, the transformation of the sample into a gel was observed. When the sample was heated for longer periods of time, more than 10 h, some precipitation was visible. Aliquots were removed at specific times after initiation of the heat treatment. All samples were centrifuged to remove any macroscopic precipitates. Analysis was then carried out on the resulting supernatant. Two different samples were prepared to follow the formation of fibrils by FTIR and EM simultaneously and for the FTIR and CD analysis. The fibrils observed in Figures 4 and 5 were formed under the conditions described above with the following modifications. The sample was prepared in H_2O and heated at 70 °C until the solution formed a gel, and then rapidly frozen in liquid nitrogen. The sample was then thawed and left at room temperature. Aliquots were removed after 10 (Fig. 4) and 40 weeks (Fig. 5).

FTIR measurements

IR spectra were recorded with a BioRad FTS-175C Fourier transform spectrometer equipped with a liquid N_2-cooled mercury cadmium telluride detector. Insulin samples were inserted between CaF_2 windows using a 50 μm Mylar spacer. Two hundred fifty interferograms were recorded at room temperature with a resolution of 2 cm^{-1}. For each spectrum, water vapor was subtracted and baseline corrected. For all spectra, the area between 1,590 and 1,710 cm^{-1} has been normalized to unity. The second derivatives, used to resolve the overlapping bands, were calculated using Grams 32 (Galactic Co., Salem, New York).

Electron microscopy

Aliquots collected at different times during fibril formation were applied to Formvar-coated grids, negatively stained with a solution of 2% (wt/vol) uranyl acetate in water, washed, air-dried, and then examined in a JEOL JEM1010 transmission electron microscope operating at an accelerating voltage of 80 kV. At longer time points, because of the large quantity of fibrils present, dilutions of the samples were carried to obtain high quality electron micrographs of the fibrils. Since it was necessary to dilute samples prior to obtaining EM pictures, it is not possible to make quantitative comparisons of the number of fibrils present under different solution conditions.

CD measurements

The CD measurements were performed on a Jasco J-720 spectropolarimeter using a cell with a 0.1 mm optical pathlength. Solvent spectra were subtracted from the measured spectra of insulin. The reported spectra are the average of two scans. The spectra have been recorded at room temperature.

X-ray diffraction

Fibre diffraction images were collected on a Cu Kα rotating anode equipped with a 180 or 345 mm MAR-Research Image plate (MAR Research, Hamburg, Germany). Oriented insulin fibrils were prepared by suspending an aliquot of the insulin sample between two wax-filled capillary ends. The distance between the capillary ends was increased in small increments to facilitate the alignment of the fibrils while drying occurred (Serpell et al., 1999). This procedure produced a small stalk of fibrils protruding from the end of one of the capillaries, which was aligned in the X-ray beam. The fibril images were analyzed using the display program IPDISP and marView run on a digital workstation (Digital Equipment Corporation, Maynard, Massachusetts).

Acknowledgments

The authors are thankful to Margaret Sunde for helpful discussions and Anne Clark for expert assistance with electron microscopy. This paper is a contribution from the Oxford Centre of Molecular Sciences, which is funded by the BBSRC, EPSRC, and the MRC. MB is grateful to the Natural Sciences and Engineering Research Council of Canada (NSERC) and to Fonds pour la Formation de Chercheurs et l'Aide à la Recherche (FCAR) of the Province of Québec for financial support. JZ is supported by a Fellowship from the European Community. EJN is grateful for financial support from Glaxo Wellcome. CVR is a Royal Society University Research Fellow. The research of CMD is supported in part by an International Research Scholars award from the Howard Hughes Medical Institute and by a Programme Grant from the Wellcome Trust.

References

Arrondo JLR, Muga A, Castresana J, Goni M. 1993. Quantitative studies of the structure of proteins in solution by Fourier transform infrared spectroscopy. *Prog Biophys Mol Biol 59*:23–56.

Blundell TL, Cutfield JF, Cutfield SM, Dodson G, Dondson GG, Hodgkin DC, Mercola DA, Vijayan M. 1971. Atomic positions in rhombohedral 2-zinc insulin crystals. *Nature 231*:506–511.

Brange J, Andersen L, Laursen ED, Meyn G, Rasmussen E. 1997a. Towards understanding insulin fibrillation. *J Pharm Sci 86*:517–525.

Brange J, Dodson GG, Edwards DJ, Holden PH, Whittingham JL. 1997b. A model of insulin fibrils derived from the X-ray crystal structure of a monomeric insulin (despentapeptide insulin). *Proteins Struct Funct Genet 27*:507–516.

Brange J, Havelund S, Hougaard P. 1992. Chemical stability of insulin. 2. Formation of higher molecular weight transformation products during storage of pharmaceutical preparations. *Pharm Res 9*:727–734.

Booth DR, Sunde M, Belloti V, Robinson CV, Hutchinson WL, Fraser PE, Hawkins PN, Dobson CM, Radford SE, Blake CCF, et al. 1997. Instability unfolding and aggregation of human lysozyme variants underlying amyloid fibrillogenesis. *Nature 385*:787–793.

Burke MJ, Rougvie MA. 1972. Cross-β protein structure. Insulin fibrils. *Biochemistry 11*:2435–2439.

Canet D, Sunde M, Last AM, Miranker A, Spencer A, Robinson CV, Dobson CM. 1999. Mechanistic studies of the folding of human lysozyme and the origin of amyloidogenic behavior in its disease-related variants. *Biochemistry 38*:6419–6427.

Chiti F, Webster P, Taddei N, Clark A, Stefani M, Ramponi G, Dobson CM. 1999. Designing conditions for in vitro formation of amyloid protofilaments and fibrils. *Proc Natl Acad Sci USA 96*:3590–3594.

Colon W, Kelly JW. 1992. Partial denaturation of transthyretin is sufficient for amyloid fibril formation in vitro. *Biochemistry 31*:8654–8660.

Dobson CM. 1999. Protein misfolding, evolution and disease. *Trends Biochem Sci 24*:329–332.

Dodson G, Steiner D. 1998. The role of assembly in insulin's biosynthesis. *Curr Opin Struct Biol 8*:189–194.

Dong A, Kendrick B, Kreilgard L, Matsuura J, Manning MC, Carpenter JF. 1997. Spectroscopic study of secondary structure and thermal denaturation of recombinant human factor XIII in aqueous solution. *Arch Biochem Biophys 347*:213–220.

Dong A, Matsuura J, Manning MC, Carpenter JF. 1998. Intermolecular β-sheet results from trifluoroethanol induced non-native α-helical structure in β-sheet predominant proteins: Infrared and circular dichroism spectroscopic study. *Arch Biochem Biophys 355*:275–281.

Fabian H, Choo L-P, Szendrei GI, Jackson M, Halliday WC, Otvos L Jr, Mantsch HH. 1993. Infrared spectroscopic characterization of Alzheimer plaques. *Appl Spectrosc 47*:1513–1518.

Gilchrist P, Bradshaw J. 1993. Amyloid formation by salmon calcitonin. *Biochem Biophys Acta 1182*:111–114.

Guijarro JI, Sunde M, Jones JA, Campbell ID, Dobson CM. 1998. Amyloid fibril formation by an SH3 domain. *Proc Natl Acad Sci USA 95*:4224–4228.

Halverson K, Fraser PE, Kirschner DS, Landsbury PT. 1990. Molecular determinants of amyloid deposition in Alzheimer's disease: Conformational studies of synthetic β-protein fragments. *Biochemistry 29*:2639–2644.

Harper J, Lansbury PT. 1997. Models of amyloid seeding in Alzheimer's disease and Scrapie: Mechanistic truths and physiological consequences of the time dependent solubility of amyloid proteins. *Annu Rev Biochem 66*:385–407.

Hua Q, Weiss MA. 1991. Comparative 2D NMR studies of human insulin and des-pentapeptide insulin: Sequential resonance assignment and implications for protein dynamics and receptor recognition. *Biochemistry 30*:5505–5515.

Jarrett JT, Lansbury PT. 1993. Seeding one dimensional crystallization of amyloid—A pathogenic mechanism in Alzheimer's disease and scrapie. *Cell 73*:1055–1058.

Jiménez JL, Guijarro JI, Orlova E, Zurdo J, Dobson CM, Sunde M, Saibil HR. 1999. Cryo-electron microscopy structure of an SH3 domain amyloid fibril and model of the molecular packing. *EMBO J 18*:815–821.

Kelly JW. 1998. The alternative conformations of amyloidogenic proteins and their multi-step assembly pathways. *Curr Opin Struct Biol 8*:101–106.

Kendrick BS, Cleland JF, Lam X, Nguyen T, Randolph TW, Manning MC, Carpenter JF. 1998. Aggregation of recombinant human interferon gamma: Kinetics and structural transition. *J Pharm Sci 87*:1069–1076.

Kirschner DA, Elliot-Bryant R, Szumowski KE, Gonnerman WA, Kindy MS, Sipe JD, Cathcart ES. 1998. In vitro amyloid formation by synthetic peptides corresponding to the amino terminus of apoSSA isoforms from mice amyloid-susceptible and amyloid-resistant mice. *J Struct Biol 124*:88–98.

Kirschner DA, Inouye H, Duffy L, Sinclair A, Lind M, Selkoe DA. 1987. Synthetic peptide homologous to β-protein from Alzheimer's disease forms amyloid-like fibrils in vitro. *Proc Natl Acad Sci USA 84*:6953–6957.

Koltun WL, Waugh DF, Bear RS. 1953. An X-ray diffraction investigation of selected types of insulin fibrils. *J Am Chem Soc 76*:413–417.

Krimm S, Bandekar J. 1986. Vibrational spectroscopy and conformation of peptides, polypeptide and proteins. *Adv Protein Chem 38*:181–364.

Lai ZH, Colon W, Kelly JW. 1996. The acid mediated denaturation pathway of transthyretin yield a conformational intermediate that can assemble into amyloid. *Biochemistry 35*:6470–6482.

Nettleton EJ, Sunde M, Lai ZH, Kelly JW, Dobson CM, Robinson CV. 1998. Protein subunit interactions and structural integrity of amyloidogenic transthyretins: Evidence from electrospray mass spectrometry. *J Mol Biol 281*:553–564.

Nettleton EJ, Tito P, Sunde M, Bouchard M, Dobson CM, Robinson CV. 2000. Characterization of the oligomeric states of insulin in self-assembly and amyloid fibril formation by mass spectrometry. *Biophys J 79*:1053–1065.

Pepys MB. 1996. Amyloidosis. In: Weatherall DJ, Ledingham JGG, Warell DA, eds. *The Oxford textbook of medicine, 3rd ed., vol 2*. Oxford, United Kingdom: Oxford University Press. pp 1512–1524.

Seilheimer B, Bohrmann B, Bondolfi L, Müller F, Stüber D, Döbeli H. 1997. The toxicity of the Alzheimer's β-amyloid peptide correlates with a distinct fiber morphology. *J Struct Biol 119*:59–71.

Serpell LC, Fraser PE, Sunde M. 1999. X-ray fiber diffraction of amyloid fbrils. *Methods Enzymol 309*:526–536.

Sipe J. 1992. Amyloidosis. *Ann Rev Biochem 61*:947–975.

Sipe J. 1994. Amyloidosis. *Clin Lab Sci 31*:325–354.

Sluzky V, Kibanov AM, Langer R. 1992. Mechanism of insulin aggregation and stabilization in agitated aqueous-solutions. *Biotechnol Bioeng 40*:895–903.

Sunde M, Blake C. 1997. The structure of amyloid fibrils by electron microscopy and X-ray diffraction. *Ad Protein Chem 50*:123–159.

Sunde M, Serpell LC, Bartlam M, Fraser PE, Pepys MB, Blake CCF. 1997. Common core structure of amyloid fibrils by synchotron x-ray diffraction. *J Mol Biol 273*:729–739

Surewicz WK, Mantsch HH, Chapman D. 1993. Determination of protein secondary structure by Fourier transform infrared spectroscopy: A critical assessment. *Biochemistry 32*:389–394.

Tan SY, Pepys MB. 1994. Amyloidosis. *Histopathology 25*:403–414.

Taubes G. 1996. Misfolding the way to disease. *Science 171*:1493–1495.

Tito P, Nettleton EJ, Robinson CV. 2000. Monitoring the conformation of insulin under amyloid fibril forming conditions: A hydrogen exchange mass spectrometry investigation. *J Mol Biol*. In press.

Turnell WG, Finch JT. 1992. Binding of the dye congo red to the amyloid protein pig insulin reveals a novel homology amongst amyloid-forming peptide sequences. *J Mol Biol 227*:1205–1223.

Vecchio G, Bossi A, Pasta PS, Carrea G. 1996. Fourier transformed infrared conformational study of bovine insulin in surfactant solutions. *Int J Peptide Protein Res 48*:113–117.

Villegas V, Zurdo J, Filimonov VV, Avilés FX, Dobson CM, Serrano L. 2000. Protein engineering as a strategy to avoid formation of amyloid fibrils. *Protein Sci 9*:1700–1708.

Waugh DF. 1946. A fibrous modification of insulin: The heat precipitate of insulin. *J Am Chem Soc 68*:247–250.

Yu NT, Jo BH, Chang RCC, Huber JD. 1974. Single-crystal Raman spectra of native insulin. Structures of insulin fibrils, glucagon fibrils, and intact calf lens. *Arch Biochem Biophys 160*:614–622.